JACS Hasina Innovations

Contents List available at JACS Directory

### Journal of Advanced Electrochemistry

journal homepage: http://www.jacsdirectory.com/jaec



# Estimation of Kinetic Parameters of the Hydrogen Insertion Reaction on AB<sub>5</sub> and AB<sub>2</sub> Alloys by Electrochemical Impedance Spectroscopy

Iva Betova\*

Department of Chemistry, Technical University of Sofia, Kl. Ohridski Blvd. 8, 1000 Sofia, Bulgaria.

#### ARTICLE DETAILS

Article history:
Received 03 November 2015
Accepted 10 November 2015
Available online 12 November 2015

Keywords: Metal hydride Electrode Impedance Spectroscopy Kinetic Model Spherical Diffusion

#### ABSTRACT

An investigation of the effect of applied potential on the impedance response of hydrogen storage alloys of the AB $_5$  (MmNi $_{3.7}$ Co $_{0.6}$ Al $_{0.4}$ Mn $_{0.3}$ ) and AB $_2$  (Ti $_{1.6}$ Vc $_{2.2}$ Zr $_{1.6}$ Ni $_{4.2}$ Cr $_{0.7}$ ) types produced by induction melting is presented. The crystallite size of the alloys was in the range of 40-60 nm as estimated by X-ray diffraction analysis. The experimental impedance spectra for the alloys as depending on potential were compared to the prediction of a generalized model of the hydrogen reaction. In the model, it has been assumed that the radius of diffusion coincides with the crystallite size of the alloys. An equivalent electrical circuit has been proposed on the basis of the transfer function of the kinetic model. By comparing the values of the equivalent circuit parameters calculated by fitting the experimental impedance spectra to the kinetic and transport equations for these parameters derived on the basis of the physical model, the parameters of the hydrogen reaction were estimated. The parameter values are discussed in terms of the influence of the structure of the alloys on their electrochemical performance in prospective nickel-hydrogen batteries.

#### 1. Introduction

The widespread use of nickel/hydride batteries is due to the recent development of multi-element multiphase metal hydride alloys with a high level of disorder. The hydrogen storage AB<sub>2</sub> -type and AB<sub>5</sub> -type alloys have been successfully used as component of the negative electrode of Ni/MH batteries [1-4]. As a result of the formation of a surface oxide layer with metallic inclusions a high catalytic activity is reached, resulting in a high specific energy and discharge capacity with a prolonged cycle life. The process of anodic polarization of metal-hydride electrodes features the following consecutive stages: diffusion of absorbed hydrogen from the bulk towards the surface, adsorption of hydrogen at the surface and an electrochemical oxidation step. The electrochemical impedance spectroscopy is one of the most employed techniques to study surface oxide layers formation on different alloys [5-7]. The kinetics of these elementary steps and the influence of different factors, e.g. the composition, the structure of the electrode, effect of electrolyte concentration on these stages are still not unambiguously clarified [8-13]. In that connection, the overall goal of the present work is to develop a theoretical model of these processes in the whole range of potentials between the cathodic and anodic limiting currents, emphasizing the region around the equilibrium potential, in which the process rate is characterized by the apparent exchange current density. More specifically, the aim is to determine the kinetic and transport parameters of the charging/discharging process of the hydride electrode by quantitative comparison of the model predictions with experimental data for the electrochemical impedance of such electrodes as depending on the type of alloy (AB<sub>5</sub> and AB<sub>2</sub>), the depth of discharge and the number of cycles. In the first part of the present paper a quantitative model of the hydride electrode based on the approach of Wang [14], takes into account the structure of the hydride electrode particles, uses spherical diffusion in the bulk of these particles at the micro-level and a distribution of conductivity in the porous structure at the macro-level is briefly described. In the second part, experimental electrochemical impedance data for metal hydride electrodes of the AB5 and AB2 types as depending on the depth of discharge and the cycle number are presented and discussed. In the third part, an attempt to estimate the basic kinetic parameters of the metalhydride electrodes of the  $AB_5$  and  $AB_2$  types is made and the significance of these parameters in view of the differences between electrode behavior are outlined.

#### 2. Experimental Methods

The preparation methods and the crystallite sizes of the two alloy types, determined using X-ray diffraction analysis, are presented in Table 1. X-ray diffraction analysis showed that the volume of the unit cell of the  $AB_2$  alloy is ca. two times larger than that of  $AB_5$ , which is a prerequisite for an easier adsorption/desorption of hydrogen in the former material. The crystallite size of the  $AB_2$  alloy is also larger (Table 1).

 $\textbf{Table 1} \ \ \text{Composition, crystallite size and preparation methods for the investigated alloys.}$ 

Alloy type	Composition	Crystallite size / nm	Method of preparation
$AB_5$	MmNi <sub>3.7</sub> Co <sub>0.6</sub> Al <sub>0.4</sub> Mn <sub>0.3</sub>	47	Induction melting
$AB_2$	Ti1.6V2.2Zr1.6Ni4.2Cr0.7	68	Induction melting

The working electrodes of the  $AB_5$  and  $AB_2$  types were disc-shaped with an area of 5.3 cm², pressed over a nickel mesh. The weight of the active mass was ca. 0.2 g. Measurements were carried out in three-electrode cell using a Pt sheet counter electrode and an HgO/Hg reference electrode. All potentials are referred to the standard hydrogen electrode (SHE). The electrolyte was 6 M KOH.

The electrodes were charged at 40-60 mA/g and discharged at 60 mA/g. The current vs. potential curves and impedance spectra were simultaneously measured in fully charged and fully discharged state at different potentials (from -1.0 to -0.55 V in fully charged state and from -0.55 to -1.0 V in fully discharged state) with an Autolab PGSTAT 30 equipped with a FRA2 module. The frequency range was 50 kHz - 0.01 Hz at an amplitude of the sine wave perturbation of 15 mV (rms). The linearity was checked by measuring spectra at amplitudes between 5 and 15 mV and the causality by a Kramers-Kronig compatibility test embedded in the commercial software. For the treatment of experimental data, a Microcal Origin platform was employed.

<sup>\*</sup>Corresponding Author
Email Address: iva\_betova@tu-sofia.bg (Iva Betova)

#### 3. Results and Discussion

#### 3.1 Current-Potential Curves

The steady-state current vs. potential curves for both charged and discharged  $AB_2$  electrode are presented in Fig. 1, whereas the corresponding curves for the  $AB_5$  electrode are shown in Fig. 2. Both electrodes are characterized by large currents of hydrogen evolution, and a response that reveals good conductivity and smaller currents in the double layer region. In general, all the electrodes produced by the method described above had reproducible electrochemical responses and were suitable for characterization with impedance spectroscopy.

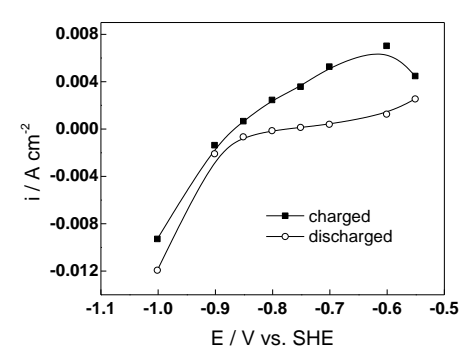


Fig. 1 Steady state current densities of a fully charged and fully discharged AB<sub>2</sub> electrode as depending on potential.

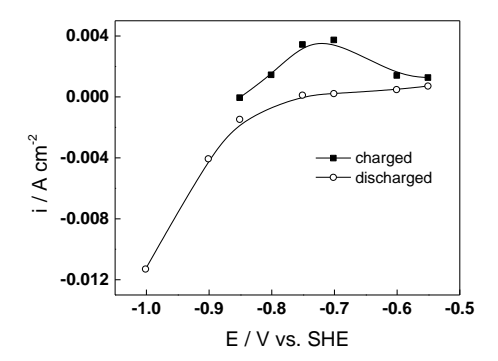


Fig. 2 Steady state current densities of a fully charged and fully discharged  $AB_{\text{\tiny 5}}$  electrode as depending on potential.

## 3.2 Impedance Spectra as Depending on the Cycle Numbed and Depth of Discharge

The impedance spectra of a fully charged and discharged  $AB_2$  electrode as depending on the cycle number, as well as the dependence of the impedance spectra on the state of discharge at the  $12^{th}$  cycle are presented in Fig. 3 and Fig. 4. The corresponding spectra for the  $AB_5$  electrode are shown in Fig. 5 and Fig. 6. The difference between the spectra is only quantitative, the impedance at lower frequency being larger in a discharged state and on the overall larger for the  $AB_2$  alloy when compared to the  $AB_5$  electrode.

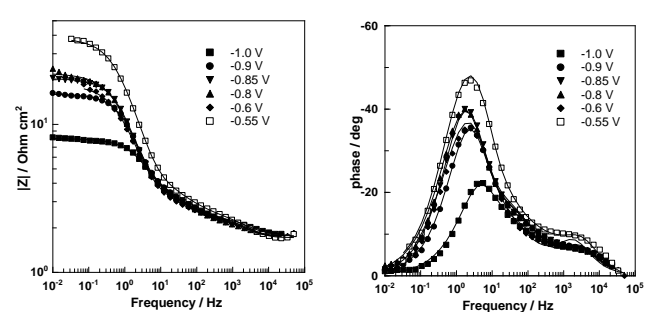
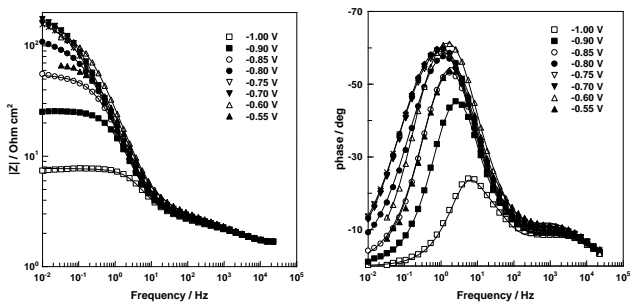


Fig. 3 Impedance spectra of a fully charged  $AB_2$  electrode as depending on potential: left - impedance magnitude vs. frequency, right – phase angle vs. frequency. Points – experimental data, solid lines – data calculated on the basis of the proposed model.

In general, it can be stated that the magnitude of the impedance at the lowest frequencies (e.g. 0.02 Hz), that can be regarded as an estimate of the polarization resistance of the electrode, is comparatively low (10-20  $\Omega cm^2$ ), when a fully charged electrode is polarized in the positive direction at potentials more negative than -0.7 V (Fig. 3), increasing steeply to 40-

 $70~\Omega cm^2$  at less negative potentials. Conversely, during polarization of a fully discharged electrode in the negative direction, the polarization resistance stays comparatively large (above  $100~\Omega cm^2)$  down to a potential of -0.85 V (close to the equilibrium potential of a fully charged electrode) (Fig. 4). It can be concluded that a significant hysteresis of the dependence of the polarization resistance on potential is observed in a potentiostatic mode of charge/ discharge. This observation is in accordance with the simultaneously measured current vs. potential curves (Figs. 1 and 2).



**Fig. 4** Impedance spectra of a fully discharged AB<sub>2</sub> electrode as depending on potential: left - impedance magnitude vs. frequency, right - phase angle vs. frequency. Points - experimental data, solid lines - data calculated on the basis of the proposed model.

The two high-frequency time constants can be related to the charge transfer (Vollmer-Heyrovsky reaction, 2-5 kHz) and the transition of hydrogen from adsorbed to absorbed state (ca. 100 Hz). On the other hand, the low-frequency time constant at 1-3 Hz can be related to the transport of hydrogen in the hydride phase in the bulk of the particles of the electrode. It can be stated that the values of the time constants at both high and low frequencies are somewhat lower for the  $AB_2\ electrode$  in comparison to AB5, i.e. the steady-state after the perturbation is reached more slowly at the AB<sub>2</sub> electrode. The spectra calculated using a non-linear regression of the experimental data with respect to the transfer function of the impedance of the hydride electrode are shown in Fig. 5 and Fig. 6 with solid lines. A very good agreement is found (the values of the  $\chi^2$ criterion were lower than 2.10-4 and those of the R2 criterion higher than 0.998), which demonstrates the ability of the model to describe adequately the experimental data for a wide combination of conditions. In general, it can be stated that the differences between the alternating current behavior of the electrodes of the two alloy types are mainly quantitative (somewhat larger total polarization resistance and slower reach of the steady state of the elementary steps at the AB2 electrode in comparison to AB<sub>5</sub>). The impedance spectra of both electrodes are adequately described by the proposed model that includes only the hydrogen insertion reaction, i.e. the side reactions can be considered negligible.

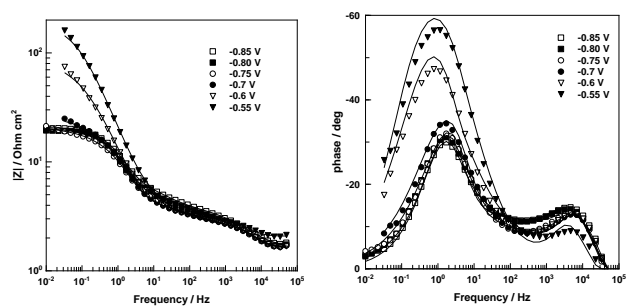


Fig. 5 Impedance spectra of a fully charged  $AB_5$  electrode as depending on potential: left - impedance magnitude vs. frequency, right – phase angle vs. frequency. Points – experimental data, solid lines – data calculated on the basis of the proposed model.

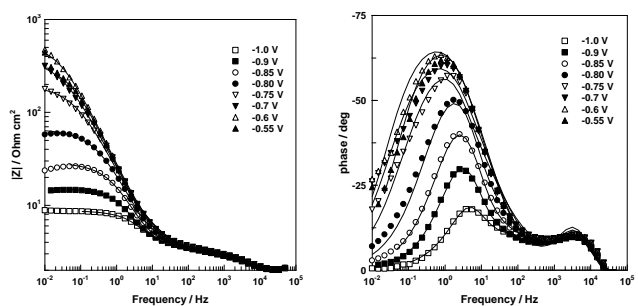


Fig. 6 Impedance spectra of a fully discharged AB<sub>5</sub> electrode as depending on potential: left - impedance magnitude vs. frequency, right - phase angle vs. frequency. Points - experimental data, solid lines - data calculated on the basis of the proposed model

(16)

The impedance spectra of a fully charged AB5 electrode as depending on the potential in the range -1.0 / -0.55 V are presented in Fig. 5 and corresponding spectra of a fully discharged AB5 electrode are shown in Fig. 6 (-0.55 / -1.0 V). The difference between the spectra for fully charged and fully discharged AB2 electrode (Fig. 3 and Fig. 4) is that the degree of reversibility of the electrode process seems greater because the hysteresis in the dependence of the polarization resistance of the potential in fully charged and fully discharged electrode is considerably smaller. Actually, in polarization of the charged electrode in a positive direction, the impedance magnitude at low frequencies increased sharply from 50 about to 200-300  $\,\Omega\text{cm}^2$  at -0.7 V (Fig. 5), while the polarization of the fully discharged electrode in negative direction, drops from 200 to about 25 Ωcm<sup>2</sup> at potential -0.8 V (Fig. 6). On the other hand, the characteristic frequencies of the three time constants are close to those of AB2 electrode (Fig. 3- Fig. 6), which once again shows that the mechanism of the overall process is qualitatively unchanged. In the following, an attempt to estimate the kinetic parameters of this process using a generalized model of the hydrogen reaction is made.

#### 3.3 Main Equations of the Model

The following reactions proceed on the metal/hydride electrode:

$$M + H_2O + e^{-} \xleftarrow{k_1} MH_{ads} + OH^{-} \text{ (charge transfer)}$$

$$MH_{ads} \xleftarrow{k_2} MH_{abs(surface)} \text{ (absorpion reaction)}$$

$$MH_{abs(surface)} \xrightarrow{J_{diff}} MH_{abs(\alpha-phase)} \text{ (spherical diffusion)}$$

$$(1)$$

According to the model of the hydrogen reaction proposed by Wang et al [14], one can write the following expression for the charge transfer reaction at open circuit under sine wave perturbation with a small amplitude

$$\vec{i} = \vec{i} = i_o = nFk_1 a_{H,O} (1 - \vec{\theta}) \exp\left(-\frac{\alpha nFE}{RT}\right) = nFk_{-1} a_{OH} - \vec{\theta} \exp\left(\frac{\beta nFE}{RT}\right)$$
(2)

If the transfer coefficients of the forward and reverse reactions are close to 0.5, and the alternating current component of the surface coverage with adsorbed hydrogen  $\theta$  is negligible face to its stationary value, the following notations can be introduced

$$A = \frac{a_{OH^{-}}}{a_{H_{2}O}} \exp\left(\frac{nFE}{RT}\right), K_{1} = \frac{k_{-1}}{k_{1}}, K_{2} = \frac{k_{-2}}{k_{2}}$$
(3)

The faradic impedance of the electrode is then

$$Z_F = Z_{ct} + Z_h \tag{4}$$

where  $Z_{ct}$  is the impedance of the charge transfer reaction, and  $Z_h$  is the impedance of the transition of hydrogen from adsorbed to absorbed state, followed by its transport in the bulk of the particle. These two impedances can be expressed as

$$Z_{ct} = \frac{RT}{nF(\alpha \vec{i} + \beta \tilde{i})} = R_t, Z_h = \frac{RT}{nF(\alpha \vec{i} + \beta \tilde{i})} \left( \frac{\vec{i}}{1 - \theta} + \frac{\vec{i}}{\theta} \right) \frac{\tilde{\theta}}{\tilde{i}}$$
(5)

The solution of (2) under sine wave perturbation with a small amplitude around the equilibrium potential gives for the charge transfer resistance

$$Z_{ct} = R_{t} = \frac{RT}{(nF)^{2} k_{-1} a_{OH}^{-} \exp\left(\frac{\beta nFE}{RT}\right)} (K_{1}A + 1)$$
(6)

To obtain an expression for  $Z_h$ , the material balances of the reaction of transition of hydrogen from adsorbed to absorbed state and the reaction of transport of hydrogen into the bulk have to be solved under sine wave perturbation with a small amplitude

$$j\omega\Gamma\tilde{\theta} = \frac{\tilde{i}}{nF} - \frac{k_2 k_{-2}\tilde{\theta}}{k_2 \overline{\theta} + k_{-2}(1 - \overline{\theta})} + [k_2 \overline{\theta} + k_{-2}(1 - \overline{\theta})]\tilde{x}_s$$

$$\tilde{i} - nF\Gamma j\omega\tilde{\theta} = nFN\tilde{x}_s f(j\omega, D)_s$$
(8)

The solution of (7)-(8) is of the type

$$\frac{\tilde{i}}{\tilde{\theta}} = \frac{nFk_2k_{-2}}{\left[k_2\bar{\theta} + k_{-2}(1-\bar{\theta})\right] \left[1 + \frac{k_2\bar{\theta} + k_{-2}(1-\bar{\theta})}{Nf(j\omega, D)_s}\right]} + j\omega\Gamma$$
(9)

where N is the total concentration of available hydrogen (molcm<sup>-3</sup>) and

$$f(j\omega,D)_{s} = \frac{\sqrt{j\omega D}}{\tanh(r_{0}\sqrt{\frac{j\omega}{D}}} - \frac{D}{r_{0}}$$
(10)

is the expression of the transport impedance for an electrode with spherical symmetry [14]. The above expression is valid for a single phase electrode, and in the present approach the shrinking core model [15] is used which includes a phase transition during the discharge. Assuming that the radius of the hydride core is not affected by the sine wave perturbation, (10) is modified as follows

$$f(j\omega,D)_{s} = \frac{\sqrt{j\omega D}}{\tanh\left[r_{0}\left[1 - \left(1 - X_{\alpha}\right)^{1/3}\right]\sqrt{\frac{j\omega}{D}}\right]} - \frac{D}{r_{0}}$$
(11)

Taking into account (5),(9) and (11), the following expression for  $Z_h$  is obtained

$$Z_{h} = \left\{ \frac{F^{2}\Gamma}{RT} \left( \sqrt{K_{1}A} + \frac{1}{\sqrt{K_{1}A}} \right)^{2} j\omega + \begin{bmatrix} \frac{RT}{(nF)^{2}k_{-2}} \left( 1 + \frac{1}{K_{1}A} \right) (1 + K_{1}K_{2}A) \\ + \left( \sqrt{K_{1}K_{2}A} + \frac{1}{\sqrt{K_{1}K_{2}A}} \right)^{2} \frac{RT}{(nF)^{2} Nf(j\omega, D)_{s}} \end{bmatrix}^{-1} \right\}^{-1}$$

$$(12)$$

The relationships between the equivalent circuit elements (Fig. 7) and the kinetic parameters in equations (6) and (12) can be written as follows

$$R_{ab} = \frac{RT}{(nF)^{2}k_{-2}} \left( 1 + \frac{1}{K_{1}A} \right) (1 + K_{1}K_{2}A)$$

$$C_{ad} = \frac{F^{2}\Gamma}{RT} \left( \sqrt{K_{1}A} + \frac{1}{\sqrt{K_{1}A}} \right)^{-2}$$

$$Z_{d} = \frac{\sigma}{\sqrt{j\omega D} \coth \left[ r_{o} [1 - (1 - X_{\alpha})^{1/3}] \sqrt{\frac{j\omega}{D}} \right] - \frac{D}{r_{o}}}$$

$$\sigma = \frac{RT}{N(nF)^{2}} \left( \sqrt{K_{1}K_{2}A} + \frac{1}{\sqrt{K_{1}K_{2}A}} \right)^{2}$$
(13)

The superposition of equations (6) and (12) can be visualized with the equivalent circuit shown in Fig. 7.

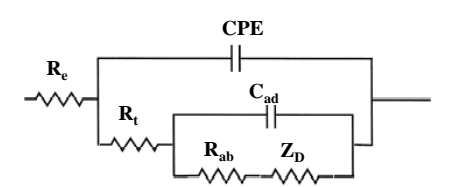


**Fig. 7** Equivalent circuit of the metal-hydride electrode. For the significance of elements, see text. The CPE is included to model the current distribution at the surface of metal-hydride particles.

#### 3.4 Comparison with Experimental Results

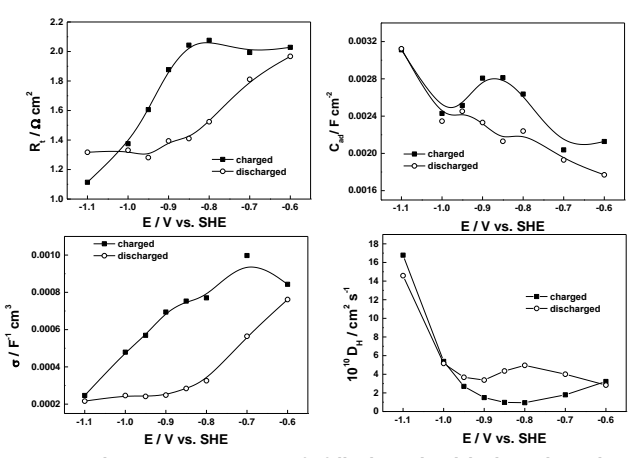


Fig. 8 Equivalent circuit parameters of a fully charged and discharged  $AB_2$  electrode as depending on potential: (above left) charge transfer resistance, (above right) adsorption pseudo-capacitance, (below left) diffusion parameter  $\sigma$  and (below right) diffusion coefficient of hydrogen in the  $\alpha$ -phase.

The values of the charge transfer resistance  $R_t$ , the adsorption pseudocapacitance  $C_{ad}$ , the diffusion parameter  $\sigma$  (Eq. 16) and diffusion coefficient of hydrogen for the  $AB_2$  electrode, obtained by non-linear regression of the experimental data with respect to the transfer function of the impedance, are presented in Fig. 8. Similar dependencies for  $AB_5$  electrode are collected in Fig. 9. It should be noted, the values of the effective radius of the diffusion is assumed to be equal to the of the crystallite sizes of the respective alloys (Table 1). It is also noted that the resistance of the hydrogen absorption reaction is calculated with a large error and thus its values are not commented further.

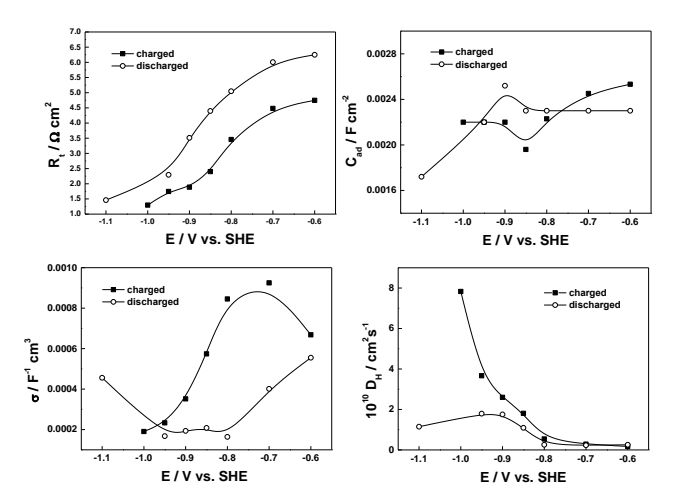


Fig. 9 Equivalent circuit parameters of a fully charged and discharged  $AB_5$  electrode as depending on potential: (above left) charge transfer resistance, (above right) adsorption pseudo-capacitance, (below left) diffusion parameter  $\sigma$  and (below right) diffusion coefficient of hydrogen in the  $\alpha$ -phase.

The dependences of the parameters  $R_t$ ,  $C_{ad}$  and  $\sigma$  on potential for the  $AB_5$  and  $AB_2$  alloys are in accordance with the predictions of equations (6), (14) and (16), i.e. the model is able to reproduce the dependence of kinetic parameters on potential. On the other hand, the diffusion coefficient of hydrogen is weakly dependent on potential, except for the most negative potentials (Fig. 8 and Fig. 9), which is also in agreement with the model concepts. At this stage, it is somewhat difficult to quantify the hysteresis observed for most of the dependences of circuit parameters on potential. In general, the hysteresis is most probably due to the occurrence of irreversible processes that accompany the charge/discharge reaction, e.g. film formation and partial blocking of adsorption sites and diffusion paths of hydrogen in the hydride particles.

To estimate the values of the kinetic parameters of the hydrogen insertion reaction (the rate constants  $k_1,k_{\cdot 1},k_2,k_{\cdot 2}$ , the diffusion coefficient of hydrogen in the bulk of the particle, the activity of hydroxyl ion at the surface  $a_{\rm OH}$  and the surface excess of adsorbed hydrogen  $\Gamma$ ) the equations (6),(13),(14) and (16) were simultaneously solved by using the mean values of the electrical circuit elements as depending on potential. The activity of water in 6 M KOH at room temperature was assumed to be 0.68 [14], and the maximal quantity of absorbed hydrogen was taken as 0.005 mol cm $^3$  (5 M). The parameters calculated on the basis of this procedure together with the crystallite size determined by X-ray diffraction are shown in Table 2.

Table 2 Kinetic parameters of the hydrogen reaction on AB<sub>5</sub> and AB<sub>2</sub> alloys.

Kinetic parameter	$AB_5$	$AB_2$	
1015 k <sub>1</sub> / cms-1	1.4	1.1	
1015 k-1 / cms-1	0.8	0.6	
106 k <sub>2</sub> / molcm <sup>-2</sup> s <sup>-1</sup>	0.9	0.5	
106 k-2 / molcm-2 s-1	9.0	6.1	
10 <sup>9</sup> Γ / molcm <sup>-2</sup>	3.3	2.5	
10 <sup>10</sup> D <sub>H</sub> / cm <sup>2</sup> s <sup>-1</sup>	3.0	4.0	
β	0.4	0.3	
106 r <sub>0</sub> / cm	4.7	6.8	

The obtained values are in good agreement with literature data for comparable electrodes [8, 14-17] which demonstrate once again the compatibility of the proposed model for the investigated systems.

#### 4. Conclusion

As a result of the present investigation, a first approach to a quantitative model of the hydrogen reaction on metal-hydride electrodes of the AB5 and AB<sub>2</sub> types, has been developed. It was based on the following processes: transfer (Vollmer-Heyrovsky reaction), a subsequent heterogeneous reaction of a transition of hydrogen from adsorbed to absorbed state and spherical diffusion of hydrogen in the crystallite bulk. X-ray diffraction data for the structure of the alloys are used to estimate the diffusion radius. The validity of the proposed approach is verified by its quantitative comparison with experimental electrochemical impedance data at open circuit as depending on the cycle number and the depth of discharge. By comparing the mean values of the equivalent electrical circuit elements with the kinetic equations, derived on the basis of the model, the kinetic and transport parameters of the hydrogen reaction have been estimated. The obtained values are in general agreement with literature data, thus the model describes adequately the discharge process of the investigated alloys and could be used for deterministic prediction of their hydrogen storage properties in a variety of conditions.

#### References

- [1] F. Ruiz, E. Castro, S. Real, H. Peretti, Electrochemical characterization of  $AB_2$  alloys used for negative electrodes in Ni/MH batteries, Int. J. Hyd. Energy 33 (2008) 3576-3580.
- [2] J. Thomas, E. Castro, A. Visintin, Influence of the compaction pressure on the electrochemical impedance spectroscopy response of the  $AB_5$ -type electrodes, Int. J. Hyd. Energy 35 (2010) 5981-5984.
- [3] M. Tliha, S. Boussami, H. Mathlouthi, J. Lamloumi, A. Percheron-Guegan, Kinetic behaviour of low-Co AB<sub>5</sub>-type metal hydride electrodes, Mater. Sci. Eng. B 175 (2010) 60-64.
- [4] F. Ruiz, H. Peretti, A. Visintin, W. Triaca, A study on  $ZrCrNiPt_x$  alloys as negative electrode components for NiMH batteries, Int. J. Hyd. Energy 36 (2011) 901-906.
- [5] C. Khaldi, H. Mathlouthi, J. Lamlouli, Electrochemical impedance spectroscopy study of the metal hydride alloy/electrolyte junction, J. Alloys Comp. 479 (2009) 284-289.
- [6] P. Slepski, K. Darowicki, M. Kopczyk, A. Sierczynska, K. Andrearczyk, Electrochemical impedance studies of AB5-type hydrogen storage alloy, J. Power Sour. 195 (2010) 2457-2462.
- [7] M. Tliha, H. Mathlouthi, J. Lamloumi, A. Percheron-Guegan, Electrochemical study of intermetallic metal hydride as an anode material for Ni–MH batteries, J. Solid State Electrochem. 15 (2011) 1963-1970.
- [8] J. Thomas, R. Humana, S. Real, R. Milocco, E. Castro, Design and optimization of single particle electrodes for the kinetic analysis of hydrogen evolution and absorption on hydrogen storage alloys, Int. J. Hyd. Energy 37 (2012) 10165-10171.
- [9] R. Humana, J. Thomas, F. Ruiz, S. Real, E. Castro, Electrochemical behavior of metal hydride electrode with different particle size, Int. J. Hyd. Energy 37 (2012) 14966-14971.
- [10] F. Ruiz, P. Martinez, E. Castro, R. Humana, H. Peretti, A. Visintin, Effect of electrolyte concentration on the electrochemical properties of an AB<sub>5</sub>-type alloy for Ni/MH batteries, Int. J. Hyd. Energy 38 (2013) 240-245.
- [11] L. Shcherbakova, M. Spodaryk, Y. Solonin, A. Samelyuk, Effects of particle size and type of conductive additive on the electrode performances of gas atomized AB<sub>5</sub>-type hydrogen storage alloy, Int. J. Hyd. Energy 38 (2013) 12133-12139.
- [12] V. Diaz, E. Teliz, F. Ruiz, P. Martinez, R. Faccion, F. Zinola, Molybdenum effect on the kinetic behavior of a metal hydride electrode, Int. J. Hyd. Energy 38 (2013) 12811-12816.
- [13] M.S. Balogun, Z. Wang, H. Chen, J. Deng, Q. Yao, H. Zhou, Effect of Al content on structure and electrochemical properties of LaNi<sub>4.4</sub> -xCo<sub>0.3</sub>Mn<sub>0.3</sub>Al<sub>x</sub> hydrogen storage alloys, Int. J. Hyd. Energy 38 (2013) 10926-10931.
- [14] C. Wang, Kinetic behavior of metal hydride electrode by means of ac impedance, J. Electrochem. Soc. 145 (1998) 1801-1812.
- [15] V.R. Subramanian, H.J. Ploehn, R.E. White, Shrinking core model for the discharge of metal hydride electrode, J. Electrochem. Soc. 147 (2000) 2868-2873.
- [16] C. Wang, M.P. Soriaga, S. Srinivasan, Determination of reaction resistances for metal-hydride electrodes during anodic polarization, J. Power Sour. 85 (2000) 212-223.
- [17] A. Lundqvist, G. Lindbergh, Kinetic study of a porous metal hydride electrode, Electrochim. Acta 43 (1999) 2523-2542.